

Molecular Pathogenesis of Genetic and Inherited Diseases

Plectin Regulates the Organization of Glial Fibrillary Acidic Protein in Alexander Disease

Rujin Tian,* Martin Gregor,[†] Gerhard Wiche,[†] and James E. Goldman[‡]

From the Department of Physiology and Cellular Biophysics* and the Department of Pathology and The Center for Neurobiology and Behavior,[‡] Columbia University, New York, New York; and the Institute of Biochemistry and Molecular Cell Biology,[†] University of Vienna, Vienna, Austria

Alexander disease (AxD) is a rare but fatal neurological disorder caused by mutations in the astrocyte-specific intermediate filament protein glial fibrillary acidic protein (GFAP). Histologically, AxD is characterized by cytoplasmic inclusion bodies called Rosenthal fibers (RFs), which contain GFAP, small heat shock proteins, and other undefined components. Here, we describe the expression of the cytoskeletal linker protein plectin in the AxD brain. RFs displayed positive immunostaining for plectin and GFAP, both of which were increased in the AxD brain. Co-localization, co-immunoprecipitation, and *in vitro* overlay analyses demonstrated direct interaction of plectin and GFAP. GFAP with the most common AxD mutation, R239C (RC GFAP), mainly formed abnormal aggregates in human primary astrocytes and murine plectin-deficient fibroblasts. Transient transfection of full-length plectin cDNA converted these aggregates to thin filaments, which exhibited diffuse cytoplasmic distribution. Compared to wild-type GFAP expression, RC GFAP expression lowered plectin levels in astrocytoma-derived stable transfectants and plectin-positive fibroblasts. A much higher proportion of total GFAP was found in the Triton X-insoluble fraction of plectin-deficient fibroblasts than in wild-type fibroblasts. Taken together, our results suggest that insufficient amounts of plectin, due to RC GFAP expression, promote GFAP aggregation and RF formation in AxD. (Am J Pathol 2006, 168:888–897; DOI: 10.2353/ajpath.2006.051028)

Glial fibrillary acidic protein (GFAP) is a member of the type III intermediate filament (IF) protein family and has long been viewed as the characteristic cytoskeletal pro-

tein of astrocytes in the central nervous system (CNS). Alexander disease (AxD) is a rare but devastating disorder of cortical white matter that predominantly affects infants and children. Neurological symptoms often include macrocephaly and episodes of severe seizures, leading to progressive disability or death within the first decade of life.¹ Pathologically, AxD is a type of leukodystrophy characterized by a loss of oligodendrocytes and the presence in astrocytes of numerous eosinophilic cytoplasmic aggregates called Rosenthal fibers (RFs). Major molecular components of RFs include GFAP itself and the small heat shock proteins α B crystallin and hsp27.² Most individuals with AxD carry missense mutations in one allele of the coding region of the *GFAP* gene.^{3,4} Our study focused on the most frequent and severe type of AxD mutation, R239C (RC) GFAP.

Plectin, a member of the plakin family of cytolinker proteins, was originally identified as an abundant IF-associated protein in C6 glioma cells⁵ and has subsequently been characterized as a ubiquitously expressed cytoskeletal cross-linker.⁶ It is localized at the cytoskeleton-plasma membrane interface and binds IFs, actin microfilaments, microtubules, and integrins. Plectin has the capacity to bridge multiple cellular structures, including sarcolemma and the Z-lines of the skeletal muscle, hemidesmosomes and focal adhesion contacts.⁷ Mutations of the human plectin gene cause autosomal recessive epidermolysis bullosa simplex, a skin blistering disorder accompanied by muscular dystrophy.⁸ Plectin knockout mice have a similar phenotype, demonstrating an important role of plectin in maintaining the structural integrity of skin and muscle.⁹

Given that a number of studies have suggested that plectin is important in the assembly and dynamics of the cytoskeleton networks in vascular and epithelial structures and in keratin-related diseases,¹⁰ we predicted that a similar association between GFAP and plectin occurred in the formation of GFAP aggregates and RFs. We there-

Supported by the National Institutes of Health (program project for cell pathology of Alexander Disease grant NS42803).

Accepted for publication November 7, 2005.

Address reprint requests to James E. Goldman, Columbia University, Department of Pathology and The Center for Neurobiology and Behavior, 630 W. 168th St., New York, NY 10032. E-mail: jeg5@columbia.edu.

fore examined plectin expression in the CNS of AxD patients. We found that plectin levels were significantly elevated in the Triton X-100 (TX)-insoluble fraction of the AxD brain tissues. Immunohistochemical staining of plectin in brain sections showed a characteristic rim staining of RFs. The interaction was further confirmed in astrocytes expressing RC GFAP as well as in immortalized fibroblasts derived from plectin (-/-) mice.

Materials and Methods

DNA Cloning

To construct N-terminally GFP- or FLAG-tagged versions of wild-type (WT) and R239C (RC) GFAP, we used the modified pcDNA3 plasmid containing a FLAG sequence (Ron Liem, Columbia University, New York, NY) and peGFP-N1 (Clontech, Palo Alto, CA). The full GFAP coding region was amplified and subcloned into the modified pcDNA3 and peGFP-N1 plasmids between the *EcoRI* and the *XhoI* sites. All plasmid inserts were fully sequenced. The *c-myc*-tagged full-length plectin (PBN165) was described previously.¹¹

Antibodies

Primary antibodies included mouse anti-GFAP monoclonal antibody (mAb 3402; Chemicon, Temecula, CA), guinea pig anti-human plectin C-terminal polyclonal antibody (Research Diagnostics, Venecia, CA), and goat anti-*c-myc* polyclonal antibody (sc-789-G; Santa Cruz Biotechnology, Santa Cruz, CA). Secondary antibodies included rabbit anti-goat IgG (H+L)-horseradish peroxidase (Southern Biotechnology, Birmingham, AL), fluorescein isothiocyanate-conjugated anti-mIgG1 (Southern Biotechnology), tetramethyl-rhodamine isothiocyanate-conjugated anti-rabbit (Chemicon), tetramethyl-rhodamine isothiocyanate-conjugated anti-guinea pig (Research Diagnostics), and horseradish peroxidase-conjugated goat anti-guinea pig (provided by Dr. Taewan Kim, Columbia University, New York, NY).

Cells, Transfection, and IF Staining

Human primary astrocytes were a gift from Dr. Paul Fisher at Columbia University, New York, NY.¹² Ple (+/+) and (-/-) immortalized fibroblasts were derived from plectin WT and knockout mice, respectively. Cells were cultured in 5% fetal calf serum in 50% Dulbecco's modified Eagle's medium-F12 medium supplemented with 50 μ g/ml each of streptomycin and penicillin. Transient transfections were performed in serum-free medium using Lipofectamine 2000 reagents (Invitrogen, Carlsbad, CA).

For indirect immunofluorescence microscopy, cells were grown on 22-mm glass coverslips. Twenty-four hours after transfection, cells were fixed in 4% paraformaldehyde for 10 to 15 minutes and subjected to indirect fluorescence/confocal laser-scanning microscopy (LSM 510 META, 100X, 1.4 N.A.; Zeiss, Thornwood, NY). All

images are projections generated from confocal serial sections of fluorescently labeled cells.

Human Brain Specimen Treatment, TX Extraction, and Immunoblotting

Frozen brain specimens of two children (control 1 and control 2) without any history of neurological or psychiatric disorder and one AxD child (R239C, RC) with a similar age were obtained at autopsy with postmortem intervals within 12 hours. Total tissue lysates were prepared from white matter homogenates of each brain by incubation for 10 minutes in sodium dodecyl sulfate-polyacrylamide gel electrophoresis (SDS-PAGE) loading buffer (62.5 mmol/L Tris-HCl, 5% SDS, 10% glycerol, 20% β -mercaptoethanol, pH 6.8) at 95°C (T: total tissue lysate; 15 μ g per lane). In certain experiments, these tissues were extracted with ice-cold TX buffer (1% TX, 50 mmol/L Tris-HCl, 100 mmol/L NaCl, pH 7.4) in the presence of protease inhibitors (Complete protease inhibitor cocktail; Roche, Indianapolis, IN). Tissue lysates were centrifuged for 10 minutes at 4°C and 15,000 \times *g*. TX-insoluble pellets were washed twice with phosphate-buffered saline and then denatured in SDS-PAGE loading buffer (P: cytoskeletal fraction; 10 μ g per lane). The TX-soluble proteins were denatured in SDS-PAGE loading buffer (S: TX-soluble fraction; 30 μ g per lane). After electrophoresis through 6% or 4 to 20% gradient Tris-bis polyacrylamide gels (Invitrogen) at 20 mA for 16 hours or 150 V for 2 hours, the separated proteins were transferred onto nitrocellulose membranes and immunostained with primary antibodies and 1:10,000 dilution of horseradish peroxidase-conjugated secondary antibodies. Reactions were visualized with an ECL kit (Amersham, Arlington Heights, IL).

Immunohistochemical Staining

Deparaffinized brain sections were incubated at room temperature in 1% H₂O₂ for 10 minutes and 0.5% NaBH₄ for 5 minutes to reduce background. Sections were then placed in blocking buffer [0.3% Triton X-100, 1% bovine serum albumin (BSA), and 5% goat serum in phosphate-buffered saline] for 2 hours and incubated overnight in guinea pig polyclonal antibody to plectin (1:200) in the same buffer. All sections were incubated with species-specific biotinylated secondary antibodies (Vector Laboratories, Burlingame, CA). The avidin-biotin immunoperoxidase method with 3,3-diaminobenzidine tetrahydrochloride was used to visualize immunoreactive cells (ABC kits, Vector Laboratories). Sufficient washes with phosphate-buffered saline were performed between each incubation step. Control sections, immunostained by the same procedure but with the omission of primary antibodies, were included in each batch of labeling. Sections with plectin labeling were examined using an Olympus BX60 microscope.

Co-Immunoprecipitation

Cells lysates were prepared 24 hours after transfection using IP buffer (10 mmol/L Tris, pH 7.4, 1.0% TX, 0.5% Nonidet P-40, 150 mmol/L NaCl, 20 mmol/L NaF, 0.2 mmol/L sodium orthovanadate, 1 mmol/L EDTA, 1 mmol/L EGTA, 0.2 mmol/L phenylmethyl sulfonyl fluoride) and centrifuged at 4°C and 15,000 × *g* for 10 minutes. Next, 200 μg of protein from the supernatant were incubated with rocking for 5 hours at 4°C with 1 μg of GFAP antibody crosslinked to protein A Sepharose-conjugated beads (Sigma Chemical Co., St. Louis, MO). The beads were washed three times with IP buffer, and antigen-antibody complexes were eluted with SDS sample buffer and analyzed by immunoblotting as described above.

In Vitro Overlay Assay

Bacteria were transformed with PET-15b (Novagen, Madison, WI)-based plasmids (modified to encode C-terminal His-tag). BN205 and BN192 encode a part of rat plectin (P30427) C-terminal domain (L3850 to A4687) and a part of plectin α-helical rod domain (E2235 to Q2577), respectively. Corresponding proteins were expressed and purified on Ni-chelating resins. Bacterially expressed WT GFAP and RC GFAP proteins were tagless and purified by high performance liquid chromatography. For overlay assays, 2 to 3 μg of BN205, BSA, WT GFAP, and RC GFAP proteins were separated on 10% polyacrylamide gels, transferred to nitrocellulose, and blocked overnight with 4% BSA in Tris-buffered saline-Tween 20 (0.1%). Blots were overlaid with BN205 and BN192 plectin recombinant proteins diluted directly from elution fractions (20 mmol/L Tris, 500 mmol/L NaCl, 6 mol/L urea, 500 mmol/L imidazol) 1:1000 in Tris-buffered saline-Tween 20 (0.1%), containing 1 mmol/L EGTA, 2 mmol/L MgCl₂, and 1 mmol/L dithiothreitol, giving the final protein concentration of 0.5 μg/ml. The assay was performed for 2 hours at room temperature. Bound proteins were detected with cell culture supernatant of myc monoclonal antibody, diluted 1:100, followed by horseradish peroxidase-conjugated goat antibodies against mouse IgGs (Jackson) diluted 1:150,000. Signal was obtained after incubation with ECL (Pierce, Rockford, IL) substrate and exposure to X-ray film.

Statistical Methods

The percentage of cells with characteristic GFAP phenotypes was quantified by randomly choosing visual fields in the fluorescence microscope and counting 150 cells per microscope slide (×40 objective). Results are expressed as means ± SEM. Each experiment was performed three times with similar results. Statistical analysis was performed using the Student's *t*-test. *P* values less than 0.05 were considered significant.

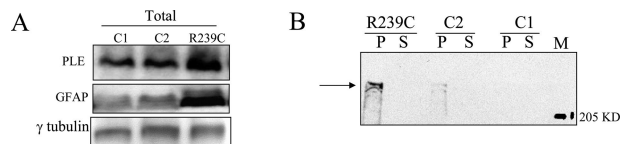


Figure 1. Immunoblot analysis of plectin in AxD and control brains. Equivalent aliquots of white matter homogenates from two control (C1 and C2) and one AxD case (R239C) were resolved on a 4 to 20% gradient gel (**A**) and 6% SDS-polyacrylamide gel (**B**). **A:** Significantly increased total amount of plectin and GFAP were found in AxD brain. **B:** Abundant plectin (between 200 and 500 kd, **arrow**) was also detected in the TX-insoluble (P) fraction of AxD brain. Position of the first molecular mass standard is indicated on the right. S, TX soluble.

Results

Plectin Is Associated with RFs: Evidence from Brain Sections and Tissues of AxD Patients

To explore the potential role of plectin in AxD, we analyzed by Western blotting the expression of plectin in white matter homogenates of an AxD patient with the RC mutation and in two control brains. The total level of plectin was dramatically increased in the AxD brain compared to both control patients. An elevated level of GFAP was also seen in the same patient (Figure 1A). Cytoskeleton-linked proteins are relatively resistant to nonionic detergent extraction, such as Triton X-100 (TX) used here. Strikingly, plectin was found to be highly enriched in the cytoskeletal fraction (P, pellet) of the AxD brain (Figure 1B). The total levels of plectin in the control patients were too low for us to compare the TX solubility of plectin in the brains of AxD and normal patients. Immunohistochemistry showed that plectin mostly co-localized with RFs in AxD brain sections (Figure 2). This co-localization was consistent with the enrichment of plectin in the cytoskeletal fraction of the AxD brain. Similar results were obtained with CNS tissues from a patient with the R416W GFAP mutation (data not shown).

Association of RC GFAP and Plectin in Human Astrocytes

To study plectin localization in human primary astrocytes, we used a polyclonal antibody that recognizes an epitope in the C-terminal domain common to many splice variants of plectin.¹³ It appeared to stain clearly the endogenous GFAP filamentous network (Figure 3, A–C) and the focal adhesion contacts and actin stress fibers in human primary astrocytes (data not shown). To compare the localization of WT versus RC GFAP in human primary astrocytes, we fused WT and RC GFAP with an N-terminal FLAG tag and transfected cells with these plasmids so the GFAP transcribed from them could be identified in the presence of the endogenous GFAP in astrocytes (Figure 3, A, D, and G; green). In human primary astrocytes transfected with WT GFAP, a fraction of the plectin was incorporated into the exogenous FLAG-tagged WT GFAP network, which appeared indistinguishable from the endogenous GFAP bundles (co-labeling with anti-FLAG and anti-GFAP antibodies; not shown). In contrast, expression of RC GFAP resulted in a complete disruption of

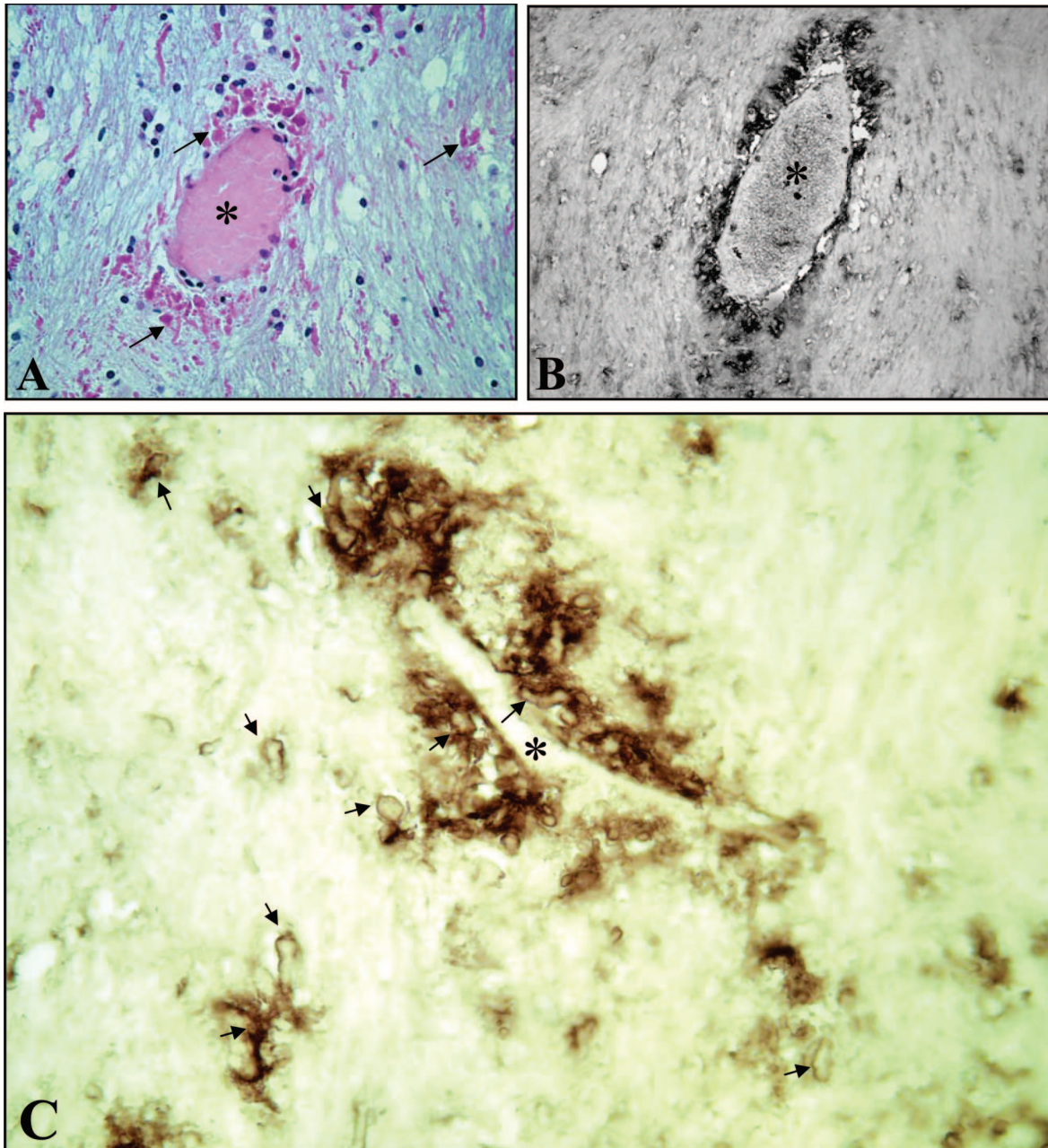


Figure 2. Plectin is associated with RFs. **A:** Characteristic pathology of AxD: copious RFs (arrows) located in the perivascular region (*, blood vessel) of the subcortical white matter (H & E). **B and C:** Immunohistochemical staining of plectin in deparaffinized brain sections of AxD. Immunoreactivity for plectin is found predominantly in the periphery of RFs (arrows) with visible staining of the RFs themselves. Original magnifications: $\times 200$ (A, B); $\times 400$ (C).

the endogenous GFAP network and concomitant redistribution of plectin into highly disorganized thin filaments and ring-shaped aggregates in a diffuse and uniform pattern throughout the cell (Figure 3, G–I), suggesting that the RC mutation is dominant.

To address further the association of plectin and RC GFAP, we generated stable transfectants expressing similar levels of GFP-GFAP fusion proteins in a human astrocytoma cell line (U251). Although it is possible that insertion of a GFP tag renders the GFAP molecule unable to polymerize properly, expression of the GFP-GFAP constructs in Cos7 cells showed staining patterns indistinguishable from those obtained with untagged versions of

GFAP (data not shown). We used nontransfected U251 cells, which contain plectin and low levels of GFAP, as a control. Cells were treated with a TX-containing buffer and the resulting extracts separated by centrifugation at $15,000 \times g$ into a pellet fraction (P, TX-insoluble cytoskeletal fraction) and a supernatant fraction (S, TX soluble). The GFAP and plectin levels in each fraction were determined by immunoblotting. We also examined the levels of plectin and GFAP in total cell lysates without TX fractionation (T, total). The total level of plectin was moderately reduced in RC GFAP stable transfectants relative to WT GFAP cells and control cells (Figure 4, left). Plectin appeared to partition differently in the two stable lines:

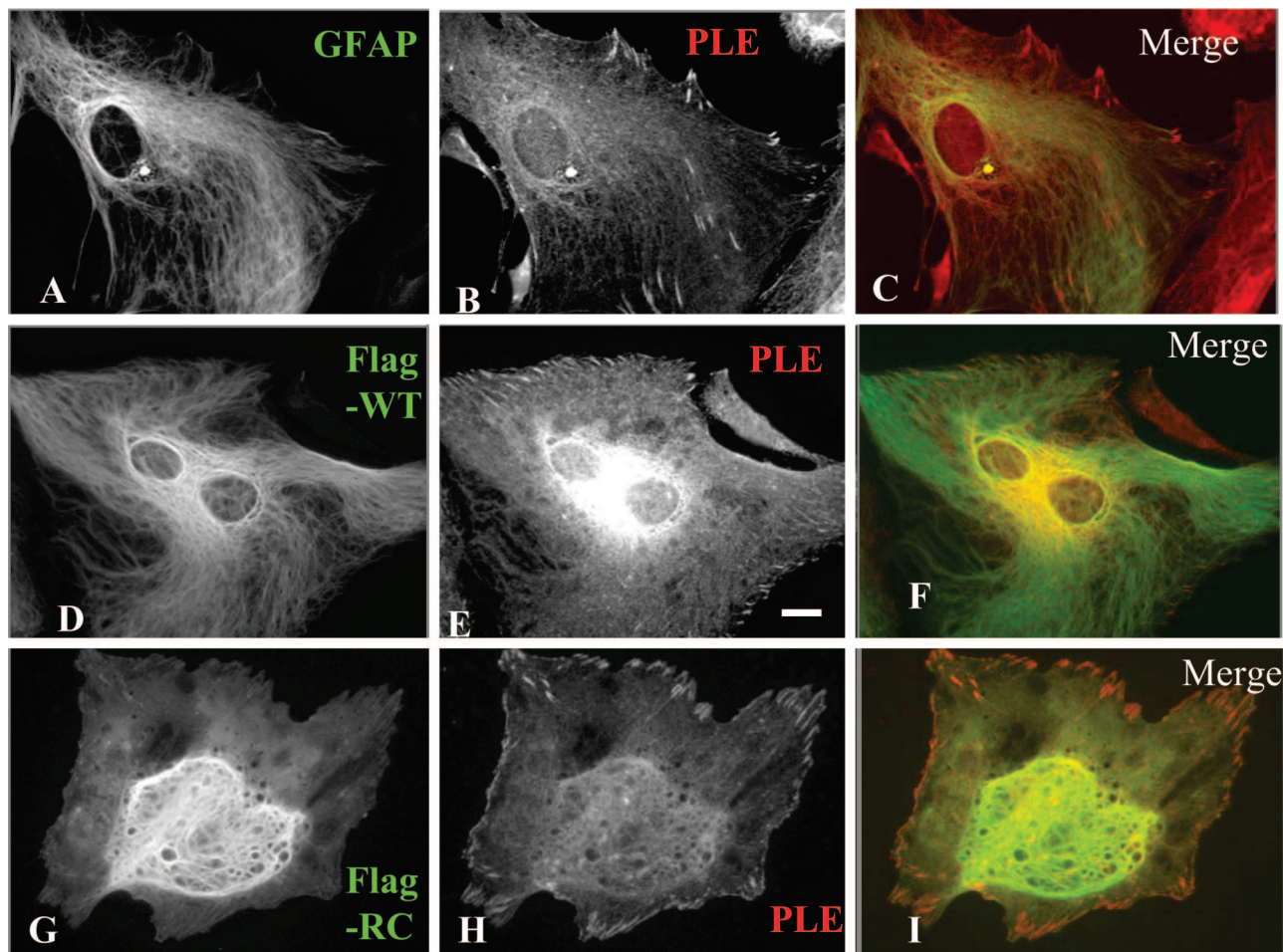


Figure 3. Localization of plectin in human astrocytes expressing GFAP. **A–C:** The localization of endogenous plectin (red) and GFAP (green) in human primary astrocytes. These cells were transiently transfected with Flag-tagged WT (**D–F**) or RC (**G–I**) GFAP and stained with anti-FLAG (green) and anti-plectin (red). The merged images (**C**, **F**, and **I**) show the degree of co-localization of plectin with GFAP. Scale bar, 10 μm .

relatively more appeared in the soluble fraction in the RC-expressing line than in the WT line, and conversely, relatively more appeared insoluble in the WT line than in the RC line (Figure 4, middle and right). In addition, relatively more RC GFAP than WT GFAP appeared in the soluble fraction (Figure 4, middle). Note that in both transfected lines, the majority of GFAP appeared in the TX-insoluble fraction (~99% of WT and 90% of RC GFAP in the TX-insoluble fraction). Thus, although plectin appears in both soluble and insoluble fractions, more plectin correlates with more RC GFAP in the soluble fraction.

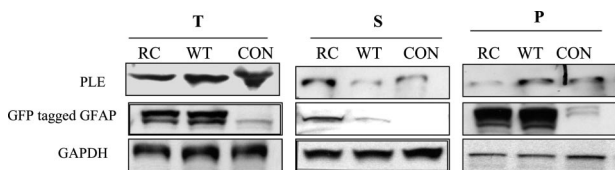


Figure 4. Immunoblot analysis in GFAP stable transfectants of U251 MG astrocytoma cells. Fifteen μg of total (T), 10 μg of high-salt/TX pellet fractions (P), and 30 μg of corresponding supernatant fractions (S) per lane were obtained from nontransfected cells (CON), WT GFAP-GFP (WT), or R239C GFAP-GFP (RC) stable transfectants.

Plectin Co-Immunoprecipitates with GFAP

We next determined whether GFAP interacted with plectin in cells. We transiently transfected fibroblasts from plectin WT (+/+) or plectin knockout (-/-) mice with WT or RC GFAP. After 24 hours, cell lysates were processed for co-immunoprecipitation using protein A-Sepharose beads loaded with anti-GFAP antibody followed by immunoblotting with anti-plectin antibody. Protein A-Sepha-

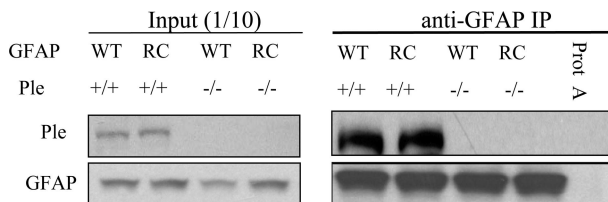


Figure 5. Plectin co-immunoprecipitates with GFAP. WT and RC GFAP were transfected into plectin (+/+) cells and plectin (-/-) cells. After 24 hours, cell lysates (200 μl) were incubated with protein A Sepharose anti-GFAP antibody, followed by Western blotting with anti-plectin antibody. WT was transfected into plectin (+/+) cells, incubated with beads without anti-GFAP antibody as a negative control (Prot A). Ten percent of the total cell lysates (input 1/10, 20 μl) was subjected to SDS-PAGE analysis and probed with anti-GFAP and anti-Ple.

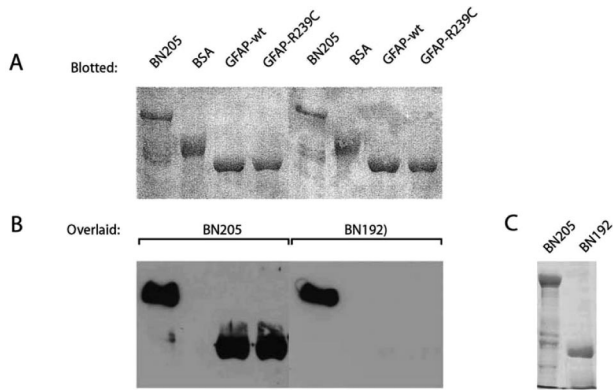


Figure 6. Blot overlay assay of GFAP and plectin. Proteins (2 to 3 mg) were separated on 10% polyacrylamide gel, blotted to the nitrocellulose (A) and overlaid with bacterially expressed plectin recombinant proteins, BN205 and BN192 (B). A: Ponceau S staining of blotted proteins. B: BN205 and BN192 were overlaid onto blotted WT GFAP and GFAP-R239C mutant protein. Bound proteins were detected with myc-tagged monoclonal antibodies. Note binding of BN205 (part of plectin C-terminal domain L3850 to A4687 including IF binding site) and not BN192 (part of a plectin α -helical rod domain E2235 to Q2577) to WT GFAP and R239C mutant. Overlaid proteins did not bind control, BSA. Lines with blotted BN205 serve as control for myc-tag detection. C: Coomassie staining of overlaid proteins.

rose beads without anti-GFAP antibodies were used as a background control (Figure 5, Prot A). As expected, plectin co-immunoprecipitated with both WT and RC GFAP in plectin (+/+) cells. Note that the IP buffer-insoluble GFAP was excluded from this assay.

Because GFAP and plectin might be associated in a co-immunoprecipitation complex consisting of multiple unidentified components *in vivo*, we used a blot overlay assay to confirm further the direct interaction *in vitro* (Figure 6). High performance liquid chromatography-purified tagless WT and RC GFAP, BN205 (a part of C-terminal

domain of rat plectin including IF binding site) and BSA (Figure 6A) were separated on SDS-polyacrylamide gels and blotted onto nitrocellulose membranes, which were then overlaid with Ni-chelating resin-purified BN205 protein. As a control, purified BN192 (a part of plectin α -helical rod domain without the IF binding site) was also overlaid with immobilized WT and RC GFAP. Bound proteins were detected by Western blot analysis using an anti-myc antibody. BN205 bound with both WT and RC GFAP to the same extent (Figure 6B).

Plectin Regulates the Organization of Both WT and RC GFAP

To test the hypothesis that plectin plays a role in regulating the organization of GFAP, we transiently transfected WT and RC GFAP into immortalized fibroblasts derived from plectin (+/+) and plectin (-/-) mice and studied the GFAP IF network by confocal immunofluorescence microscopy. We found that WT GFAP alone can form a normal bundled filamentous network (Figure 7A). The loss of plectin appeared to impair partially the organization of WT GFAP, resulting in short-filament aggregates and densely packed perinuclear bundles in ~60% of the WT-transfected cells (Figure 7B). In contrast, RC GFAP was unable to organize into bundled filaments in plectin-expressing cells and instead formed disorganized, thin filaments in a diffuse pattern (Figure 7C and Figure 8A). Plectin showed primarily a filamentous staining and co-localized with RC GFAP (Figure 8A, red). A majority of plectin-negative fibroblasts transfected with RC GFAP showed characteristic ring-shaped aggregates (Figure 7D and Figure 8B).

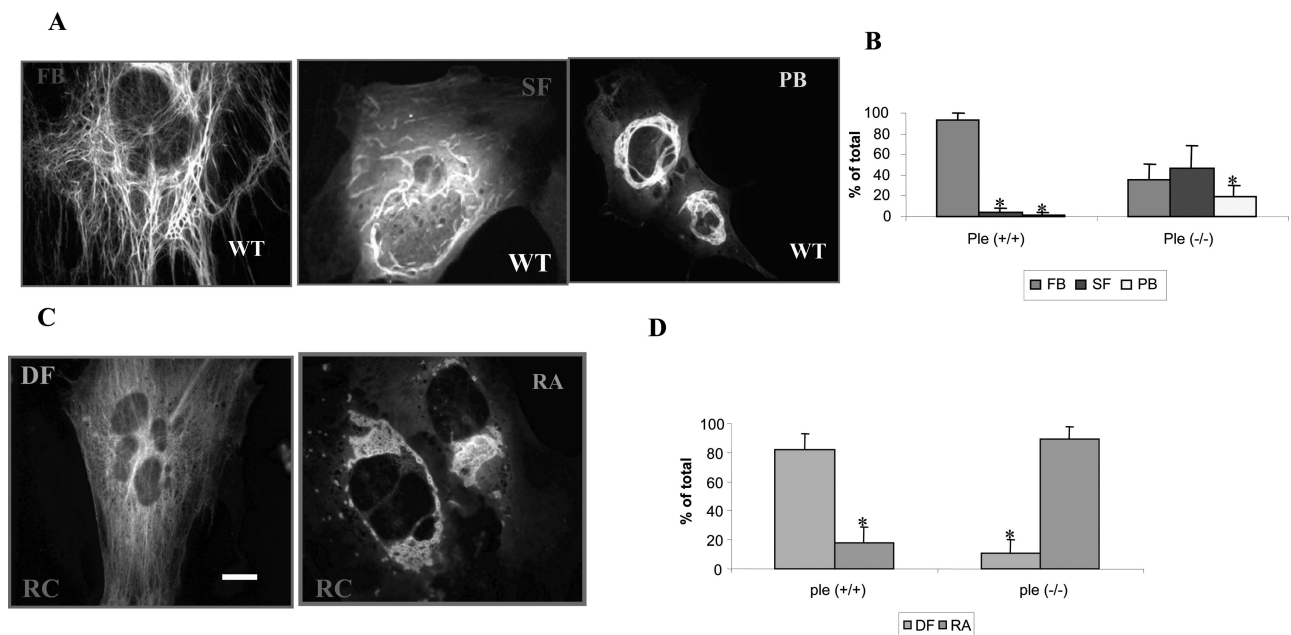


Figure 7. GFAP organization in plectin (+/+) and plectin (-/-) cells. WT (A) or RC (C) GFAP were transiently transfected into mouse fibroblasts (either plectin-positive or -negative). The WT-transfected cells displayed the following GFAP phenotypes: filamentous bundles (FB), short filaments (SF), and perinuclear bundles (PB). The RC-transfected cells displayed either a diffuse filament (DF) phenotype or a ring-shaped aggregate (RA) phenotype. B and D: The quantitative distributions of each phenotype in plectin-positive and -negative cells. An asterisk indicates the difference compared with other patterns within each group is statistically significant ($P < 0.05$). Scale bar, 10 μ m.

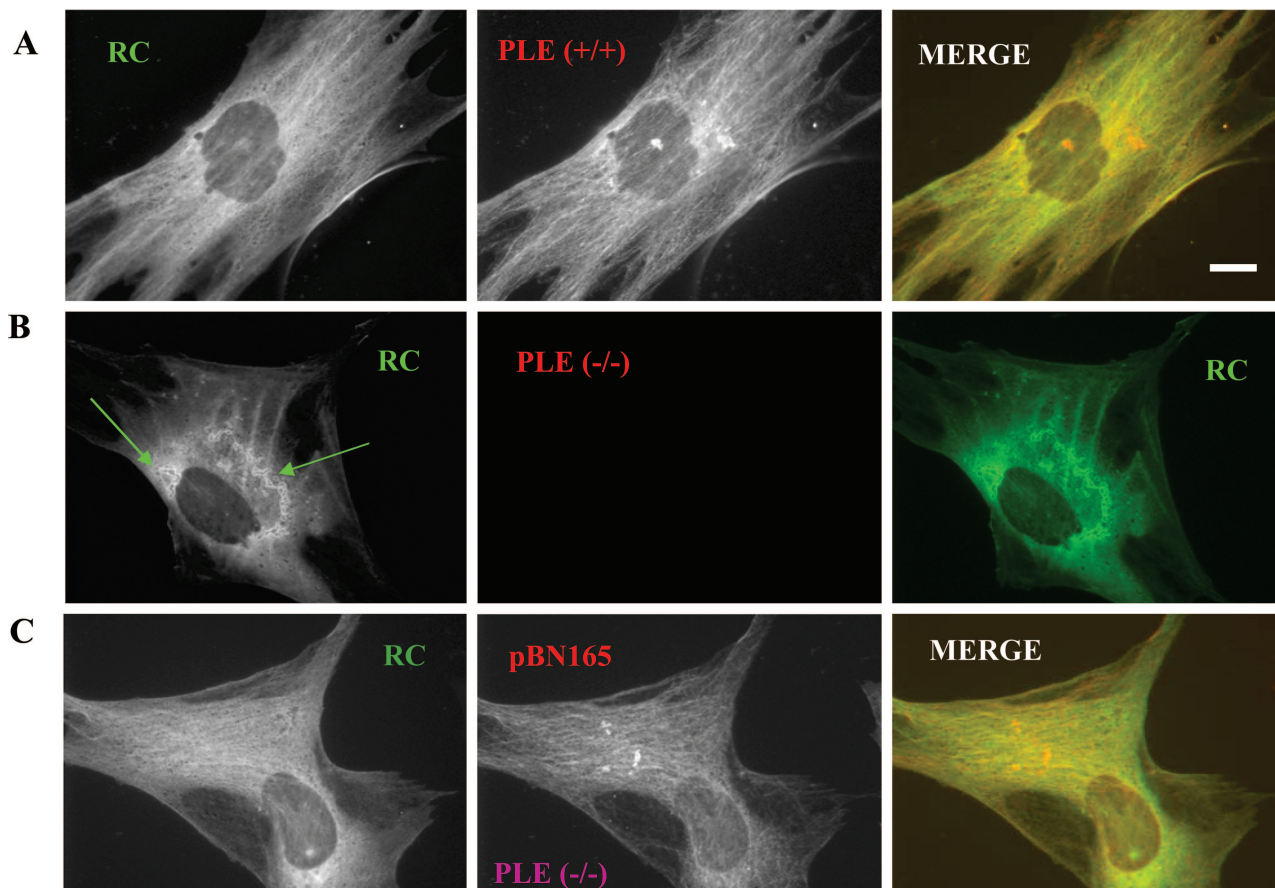


Figure 8. Co-expression of mutant GFAP and full-length plectin in plectin (-/-) cell. **A:** R239C GFAP in plectin (+/+) cells showed disorganized thin filaments. Green is GFAP, red is Ple. **B:** R239C GFAP formed ring-shaped aggregates in plectin (-/-) cells. **Arrowheads** indicate the characteristic ring-shaped aggregates. **C:** Reorganization of mutant GFAP filaments by co-transfecting a *c-myc*-tagged full-length plectin (pBN165) with the mutant GFAP in plectin (-/-) cells. Scale bar, 10 μ m.

These observations indicate that plectin is critically important for RC GFAP to form a well-spread filamentous pattern. Consistent with this finding, reintroduction of full-length plectin into plectin-null cells by transient transfection rescued the RC GFAP aggregates and resulted in thin filament formation (Figure 8C).

Comparison of WT and RC GFAP Redistribution in Plectin-Null Cells

The observation that organization of RC GFAP appears to be more severely impaired in the absence of plectin (Figure 7D) prompted us to examine the effect of plectin depletion on the partitioning of RC GFAP between TX-soluble and -insoluble fractions. As shown in Figure 9A, plectin depletion did not significantly alter the total amount of GFAP (T, total). However, the presence of plectin altered the partitioning of GFAP between soluble (S) and pellet (P) fractions. In plectin-expressing cells, a higher amount of both WT and RC GFAP was found in the TX-soluble fraction (S) compared with that observed in the same fraction of plectin-null cells. As expected, a greater amount of WT and RC GFAP was found in the TX-insoluble (P) fraction in plectin-null cells than in plectin-expressing cells. These data suggest that plectin is

able to shift GFAP from the TX-insoluble fraction to the TX-soluble fraction. In the absence of plectin, the redistribution of RC GFAP to the TX-insoluble fraction was more remarkable than that of WT GFAP (P, middle panel).

Consistent with our findings in the RC GFAP stable transfectants (Figure 4, T), plectin-positive fibroblasts expressing RC GFAP also showed a lower level of total plectin (Figure 9, T) and a higher level of TX-soluble plectin (Figure 9, S) compared to those observed in cells expressing WT GFAP. To clarify further the effect of RC GFAP expression on the total level of plectin, we again used immunoblotting to detect the endogenous plectin in untransfected (Utxf), WT-, and RC GFAP-transfected plectin-positive cells at 24 hours after transfection (Figure 9B). No differences were observed between the amount of plectin in cells overexpressing WT GFAP and untransfected control cells, but cells expressing RC GFAP contained significantly less plectin, suggesting that abnormal organization of RC GFAP may be due in part to a significantly lower plectin level.

Effect of Plectin on RC GFAP Filament Organization

Our immunofluorescence studies showed that in the presence of endogenous plectin the organization of RC

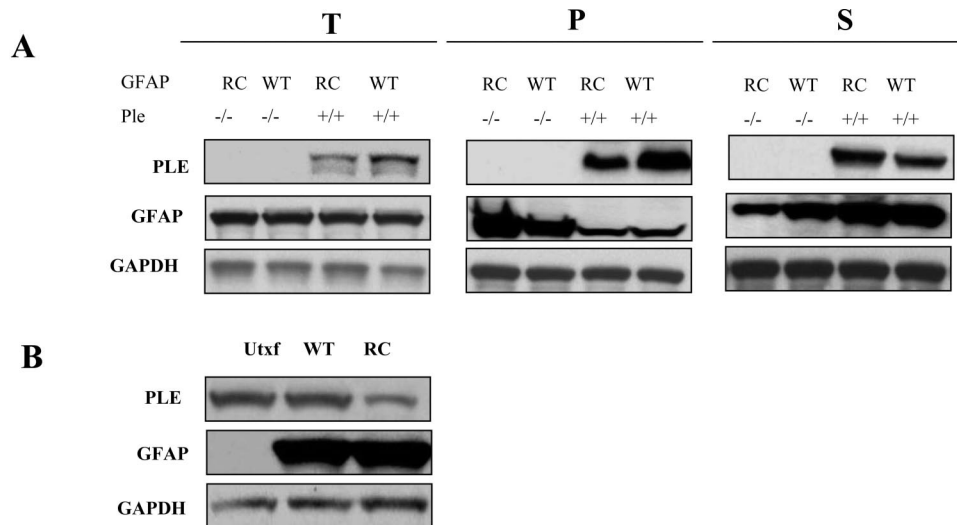


Figure 9. TX fractionation of GFAP in plectin (+/+) and (-/-) cells. **A:** Immunoblot analysis of detergent-fractionated proteins from plectin (+/+) and (-/-) cells transfected with WT and RC GFAP. Equal amounts of total protein (T, 15 mg), TX-extracted (S, soluble; 50 μ g), and nonextracted (P, pellet; 10 μ g) fractions were detected by immunoblotting using anti-GFAP and anti-plectin antibodies. **B:** Comparison of total level of plectin in untransfected (UTxf), WT GFAP (WT), and RC GFAP (RC) transfected plectin (+/+) cells.

GFAP was quite different in plectin-positive fibroblasts (Figure 8A) from that observed in primary human astrocytes (Figure 3G). To explain these disparate findings, we performed immunoblot analysis of plectin in plectin-positive fibroblasts, human primary astrocytes, and plectin-null fibroblasts without introducing any GFAP proteins (Figure 10A). Compared to human primary astrocytes, plectin-positive fibroblasts possessed a significantly greater level of endogenous plectin, suggesting that RC GFAP formed a more organized filamentous structure in the cellular context of higher plectin. To confirm the conclusion further, we co-transfected human primary astrocytes with Flag-tagged RC GFAP and pBN165. The co-transfected cells showed a striking change in RC GFAP organization, compared to cells transfected with RC GFAP only (Figure 3G). On co-transfection with pBN165, RC GFAP formed a diffuse pattern of cytoplasmic thin filaments resembling that seen in plectin (+/+) fibroblasts (Figure 10, B and C). Approximately 50% of the co-transfected cells exhibited a punctate perinuclear staining of RC GFAP co-existing with the uniformly diffuse filamentous pattern (Figure 10C), suggesting that RC GFAP can form aggregates even in the presence of high levels of plectin.

Discussion

Although the role of protein aggregation in neurodegenerative disorders remains highly controversial,¹⁴ it is generally agreed that intracellular protein aggregates are formed by the selective and robust sequestration of other proteins that may normally interact with the causal protein. Accordingly, our original interest in plectin arose from three observations. First, plectin functions as a versatile cytoskeletal linker protein.¹⁰ Second, plectin deficiency in humans results in a pathological condition called epidermolysis bullosa simplex with muscular dys-

trophy,¹⁵ which is characterized by the disorganization of the desmin cytoskeleton. Third, plectin is abundant in reactive astrocytes of the CNS.^{16,17} We started our study by examining the presence of plectin in AxD brain sections and tissues. Anti-plectin antibodies co-localized with RFs in AxD brain sections, and the AxD brain tissues showed a substantial increase of plectin in the TX-insoluble fractions, strongly suggesting that plectin is in close association with RFs. We confirmed the association of plectin and GFAP by cell staining. GFAP and plectin exhibited a significant degree of co-localization in transiently transfected human primary astrocytes and mouse fibroblasts. Furthermore, co-immunoprecipitation of plectin with anti-GFAP antibodies and detection of GFAP-plectin binding in an *in vitro* overlay assay demonstrated that the interaction of plectin and GFAP is likely to be direct.

Plectin Promotes Extended Filamentous Organization of Both WT and RC GFAP

Plectin-deficient mouse fibroblasts have allowed us to address directly the role of plectin in GFAP organization.¹⁸ In the absence of plectin, some WT and the vast majority of RC GFAP appeared to form perinuclear bundles, short-filament aggregates or ring-shaped aggregates throughout the cytoplasm. Reintroduction of full-length plectin by transient transfection primarily converted them to a diffuse filamentous organization similar to that observed in plectin-positive fibroblasts. These observations are consistent with the established role of plectin in promoting IF organization, probably by attaching IF filaments to the cell periphery or interlinking IFs and other cytoskeletal elements in skin and muscles.¹⁰

To test whether plectin could act in a similar manner in human primary astrocytes, where the aggregation of GFAP occurs in AxD, we co-transfected a *c-myc*-tagged

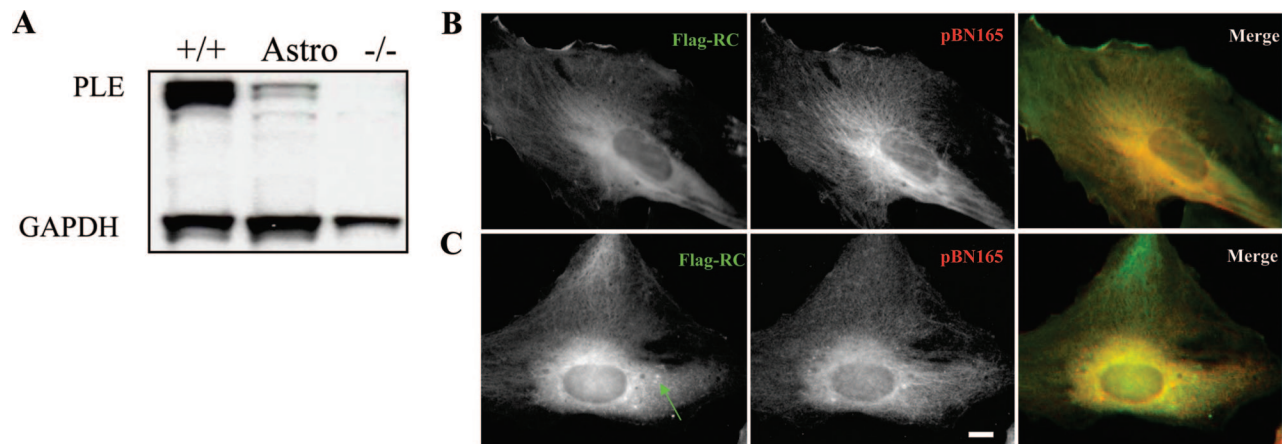


Figure 10. RC GFAP organization and plectin levels in human primary astrocytes. **A:** Detection of endogenous plectin in plectin-positive fibroblasts (+/+), human primary astrocytes (Astro), and plectin-null fibroblasts by immunoblotting. **B and C:** Human primary astrocyte cells were co-transfected with expression vectors encoding Flag-tagged RC GFAP and a *c-myc*-tagged full-length plectin (pBN165). At 24 hours after transfection, cells were stained with anti-Flag (green) and anti-*c-myc* (red). Two examples of co-transfected cells (**B, C**) display diffuse filamentous GFAP staining in the periphery of the cytoplasm and an intense perinuclear staining. Punctate perinuclear staining was evident in ~50% of these cells (**C, arrowhead**). Scale bar, 10 μ m.

full-length plectin and a Flag-tagged RC GFAP into human primary astrocytes. Compared to the aberrant organization in cells transfected only with RC GFAP, most co-transfected astrocytes exhibited uniformly distributed thin filaments of RC GFAP. Thus, plectin can promote a spread GFAP organization. The endogenous plectin levels in astrocytes are much lower than those in plectin-positive fibroblasts, suggesting that the ratio of plectin to GFAP is an important determinant of IF organization (see below). In the rat CNS plectin has been located on fine filamentous structures lying between GFAP filaments and the submembrane region at the astrocytic end-feet abutting on blood vessels and on the pial surface.¹⁹ Plectin may mediate the attachment of GFAP to the cell cortex, presumably to help maintain the filamentous organization of GFAP in astrocytes.

Cellular Context Is Important for the Organization and TX Solubility of GFAP

The varying organization and TX solubility of GFAP in different cell types is likely caused by the relative levels of co-assembly partners and interlinking proteins such as vimentin and plectin present in different cellular contexts. The ratio of plectin to GFAP in different cell types appears to be a good indicator of the organization of GFAP, especially RC GFAP. Lower plectin/GFAP ratios favor GFAP aggregation; higher ratios, extended filament formation. Thus, RC GFAP formed abnormal aggregates without obvious filamentous structure in human primary astrocytes and plectin-null fibroblasts. However, in plectin-null fibroblasts and in primary astrocytes transfected with full-length plectin to increase the plectin/GFAP ratio, RC GFAP mainly exhibited diffuse thin filaments resembling those seen in plectin (+/+) fibroblasts.

The TX solubility of GFAP also varies considerably among different cell types. RC GFAP displayed a more TX-soluble profile (monomers or short filaments do not

sediment at 15,000 \times g) than WT GFAP in human astrocytoma-derived stable transfectants. In contrast, we observed a significantly greater fraction of TX-insoluble RC GFAP in plectin-null fibroblasts and IF-free SW13 cells transiently transfected with RC GFAP.²⁰ Studies in primary astrocytes derived from RC GFAP transgenic mice will be required to confirm the larger TX-soluble pool detected in the human stable transfectants.

Implications for IF Disorganization in AxD

Human primary astrocytes with a relatively low endogenous level of plectin formed disorganized RC GFAP aggregates, which were converted to a more well spread filamentous-looking pattern through co-transfection of full-length plectin and RC GFAP in these cells. Therefore, RC GFAP does not form the bundled filaments typical of WT GFAP networks regardless of the abundance of plectin in human astrocytes. Because the RC mutation is located in the 2A region of the highly conserved rod domain, we speculate that the mutation impairs the helix-helix interactions of the GFAP coiled-coil dimer, resulting in a reduction of the higher-order polymerization of filaments into a closely packed filamentous network. *In vitro* assembly studies and electron microscopy analyses have shown that RC GFAP is able to form normal-appearing IFs.²⁰ However, unlike IF assembly *in vitro*, *in vivo* assembly is mediated by such various factors as phosphorylation state and the availability of cytoskeletal linker proteins such as plectin.²¹ Although we found in a blot overlay assay that plectin binds to WT and RC GFAP monomers with similar affinities, we do not know if RC GFAP filaments bind plectin as well as do WT GFAP filaments.

We also noticed that expression of RC GFAP results in decreased levels of endogenous plectin in both human astrocytoma-derived stable transfectants and plectin (+/+) fibroblasts. In contrast, plectin levels

remained unchanged in the untransfected controls and WT transfectants. We were unable to confirm this finding of reduced plectin expression in frozen brain tissues of AxD patients. However, we do not know the numbers of astrocytes in the tissues, the ratio of WT to RC GFAP proteins in these astrocytes, and the effects of storage at low temperature on plectin solubility, all variables that could alter plectin levels with respect to other proteins. Examination of AxD brain sections and tissues showed that astrocytes in the subcortical white matter area accumulate more GFAP and GFAP assembly regulatory proteins such as α B crystallin and plectin.²² The organization of GFAP, including both WT and RC GFAP, might be highly dependent on the ratio of GFAP assembly regulatory proteins to GFAP in astrocytes. A lower plectin/GFAP ratio, resulting from the reduced level of total plectin in response to RC GFAP expression in astrocytes, would promote the abnormal organization and aggregation of GFAP into RFs in AxD.

Pathology in the CNS has been linked to a plectin mutation. The C-terminal domain of plectin consists of six highly conserved repeats, and the IF-binding domain of plectin has been mapped to a short segment between repeats 5 and 6.²³ A homozygous insertion close to the IF-binding domain of plectin has been linked to epidermolysis bullosa simplex-muscular dystrophy in at least one patient who presented with marked desmin accumulations in muscle tissue and severe cerebral atrophy.¹⁵ Combined with other case reports of brain atrophy associated with epidermolysis bullosa simplex,^{24,25} this suggests that perturbations of the plectin/IF interactions due to plectin mutations or IF mutations can lead to neurological pathology.

Acknowledgments

We thank Dr. Albee Messing, Dr. Michael Brenner, and Dr. Ron Liem for reviewing the manuscript and critical discussions; and Dr. Tae-wan Kim, Dr. Paul Fisher, and Dr. Guomei Tang for kindly providing reagents and human astrocytes.

References

- Messing A, Goldman JE, Johnson AB, Brenner M: Alexander disease: new insights from genetics. *J Neuropathol Exp Neurol* 2001, 60:563–573
- Goldman JE, Corbin E: Isolation of a major protein component of Rosenthal fibers. *Am J Pathol* 1988, 130:569–578
- Brenner M, Johnson AB, Boespflug-Tanguy O, Rodriguez D, Goldman JE, Messing A: Mutations in GFAP, encoding glial fibrillary acidic protein, are associated with Alexander disease. *Nat Genet* 2001, 27:117–120
- Rodriguez D, Gauthier F, Bertini E, Bugiani M, Brenner M, N'Guyen S, Goizet C, Gelot A, Surtees R, Pedespan JM, Hernandez X, Troncoso M, Uziel G, Messing A, Ponsot G, Pham-Dinh D, Dautigny A, Boespflug-Tanguy O: Infantile Alexander disease: spectrum of GFAP mutations and genotype-phenotype correlation. *Am J Hum Genet* 2001, 69:1134–1140
- Wiche G, Herrmann H, Leichtfried F, Pytela R: Plectin: a high-molecular-weight cytoskeletal polypeptide component that copurifies with intermediate filaments of the vimentin type. *Cold Spring Harb Symp Quant Biol* 1982, 46:475–482
- Herrmann H, Wiche G: Plectin and IFAP-300K are homologous proteins binding to microtubule-associated proteins 1 and 2 and to the 240-kilodalton subunit of spectrin. *J Biol Chem* 1987, 262:1320–1325
- Steinbock FA, Wiche G: Plectin: a cytolinker by design. *Biol Chem* 1999, 380:151–158
- Uitto J, Pulkkinen L: Molecular complexity of the cutaneous basement membrane zone. *Mol Biol Rep* 1996, 23:35–46
- Andra K, Lassmann H, Bittner R, Shorny S, Fassler R, Propst F, Wiche G: Targeted inactivation of plectin reveals essential function in maintaining the integrity of skin, muscle, and heart cytoarchitecture. *Genes Dev* 1997, 11:3143–3156
- Wiche G: Role of plectin in cytoskeleton organization and dynamics. *J Cell Sci* 1998, 111:2477–2486
- Nikolic B, MacNulty E, Mir B, Wiche G: Basic amino acid residue cluster within nuclear targeting sequence motif is essential for cytoplasmic plectin-vimentin network junctions. *J Cell Biol* 1996, 134:1455–1467
- Su ZZ, Kang DC, Chen Y, Pekarskaya O, Chao W, Volsky DJ, Fisher PB: Identification of gene products suppressed by human immunodeficiency virus type 1 infection or gp120 exposure of primary human astrocytes by rapid subtraction hybridization. *J Neurovirol* 2003, 9:372–389
- Stegh AH, Herrmann H, Lampel S, Weisenberger D, Andra K, Seper M, Wiche G, Krammer PH, Peter ME: Identification of the cytolinker plectin as a major early in vivo substrate for caspase 8 during CD95- and tumor necrosis factor receptor-mediated apoptosis. *Mol Cell Biol* 2000, 20:5665–5679
- Bossy-Wetzel E, Schwarzenbacher R, Lipton SA: Molecular pathways to neurodegeneration. *Nat Med* 2004, 10:S2–S9
- Schroder R, Kunz WS, Rouan F, Pfendner E, Tolksdorf K, Kappes-Horn K, Altenschmidt-Mehring M, Knoblich R, van der Ven PF, Reimann J, Furst DO, Blumcke I, Vielhaber S, Zillikens D, Eming S, Klockgether T, Uitto J, Wiche G, Rolfs A: Disorganization of the desmin cytoskeleton and mitochondrial dysfunction in plectin-related epidermolysis bullosa simplex with muscular dystrophy. *J Neuropathol Exp Neurol* 2002, 61:520–530
- Lie AA, Schroder R, Blumcke I, Magin TM, Wiestler OD, Elger CE: Plectin in the human central nervous system: predominant expression at pia/glia and endothelia/glia interfaces. *Acta Neuropathol (Berl)* 1998, 96:215–221
- Kalman M, Szabo A: Plectin immunopositivity appears in the astrocytes in the white matter but not in the gray matter after stab wounds. *Brain Res* 2000, 857:291–294
- Andra K, Nikolic B, Stocher M, Drenckhahn D, Wiche G: Not just scaffolding: plectin regulates actin dynamics in cultured cells. *Genes Dev* 1998, 12:3442–3451
- Nakazawa E, Ishikawa H: Ultrastructural observations of astrocyte endfeet in the rat central nervous system. *J Neurocytol* 1998, 27:431–440
- Hsiao VC, Tian R, Long H, Perg MD, Brenner M, Quinlan RA, Goldman JE: Alexander-disease mutation of GFAP causes filament disorganization and decreased solubility of GFAP. *J Cell Sci* 2005, 118:2057–2065
- Portet S, Vassy J, Hogue CW, Arino J, Arino O: Intermediate filament networks: in vitro and in vivo assembly models. *C R Biol* 2004, 327:970–976
- Head MW, Hurwitz L, Kegel K, Goldman JE: AlphaB-crystallin regulates intermediate filament organization in situ. *Neuroreport* 2000, 11:361–365
- Steinbock FA, Nikolic B, Coulombe PA, Fuchs E, Traub P, Wiche G: Dose-dependent linkage, assembly inhibition and disassembly of vimentin and cytokeratin 5/14 filaments through plectin's intermediate filament-binding domain. *J Cell Sci* 2000, 113:483–491
- Kletter G, Evans OB, Lee JA, Melvin B, Yates AB, Bock HG: Congenital muscular dystrophy and epidermolysis bullosa simplex. *J Pediatr* 1989, 114:104–107
- Doriguzzi C, Palmucci L, Mongini T, Bertolotto A, Maniscalco M, Chiado-Piat L, Zina AM, Bundino S: Congenital muscular dystrophy associated with familial junctional epidermolysis bullosa letalis. *Eur Neurol* 1993, 33:454–460